

Ultrahigh harmonics from laser-assisted ion-atom collisions

Manfred Lein and Jan M. Rost

Max Planck Institute for the Physics of Complex Systems,
Nöthnitzer Straße 38, D-01187 Dresden, Germany

(Dated: June 26, 2018)

We present a theoretical analysis of high-order harmonic generation from ion-atom collisions in the presence of linearly polarized intense laser pulses. Photons with frequencies significantly higher than in standard atomic high-harmonic generation are emitted. These harmonics are due to two different mechanisms: (i) collisional electron capture and subsequent laser-driven transfer of an electron between projectile and target atom; (ii) reflection of a laser-driven electron from the projectile leading to recombination at the parent atom.

PACS numbers: 42.65.Ky,34.50.Rk,32.80.Rm,34.70+e

Over the last decades, a vast amount of work has been devoted to the study of ion-atom collisions [1] and atoms in intense laser fields [2, 3]. However, the two areas were almost entirely separated. No experiments on ion-atom collisions in the presence of strong laser pulses have been carried out. The reported experiments on laser-assisted collisions [4] involve one-photon processes and thermal collision energies. Also, theoretical descriptions [5] have mostly been limited to slow collisions and/or relatively weak fields. Recently, however, the theoretical works by Madsen *et al.* [6] and by Kirchner [7] investigate fast collisions in the presence of a strong laser field. In Ref. [6], excitation mechanisms are discussed, while Ref. [7] focuses on ionization and electron capture. In both cases, the presence of the field leads to a significant modification of the collision process. On the other hand, there has been no study on the question how typical strong-field processes in atoms, such as high-order harmonic generation (HHG) [8] and above-threshold ionization [9], are modified due to the impact of an ion projectile. In HHG, a large number of incoming laser photons are converted into a single high-energy photon. HHG experiments are presently pursued with great effort [10, 11] since the process serves as a source of coherent XUV radiation and attosecond pulses.

In the present work, we investigate HHG in laser-assisted ion-atom collision. We focus on impact velocities such that the time-scales of nuclear and electronic motion are comparable, i.e., we have significant probabilities for collisional electron transfer from the target to the projectile. For sufficiently long laser pulse durations, the laser-driven electron effectively sees a large range of internuclear distances during one laser pulse. When the laser polarization axis is parallel to the ion impact velocity, we show that this situation results in the generation of high harmonics with photon energies much higher than usually obtained in atomic HHG.

The classical recollision model [12] describes atomic HHG as a sequence of strong-field ionization, acceleration of the electron in the laser field and recombination with the core. Within this model, the maximum re-

turn energy of the laser-driven electron is $3.17U_p$ where $U_p = E_0^2/(4\omega^2)$ is the ponderomotive potential for a laser with field amplitude E_0 and frequency ω . The maximum energy of the emitted photons is then equal to $3.17U_p + I_p$ where I_p is the atomic ionization potential. For ion-atom collisions, we show below how the interplay between collisional electron capture and laser-driven electron transfer between target and projectile leads to new mechanisms of HHG with cutoffs at significantly higher energies.

We consider collisions of protons on hydrogen atoms for proton energies of 2 keV (impact velocity $v = 0.283$ a.u.). Due to the large impact momentum, the projectile trajectory is assumed to be classical and along a straight line. Furthermore, we use a two-dimensional model where all dynamics is restricted to the plane that contains the target nucleus and the projectile. The internuclear vector is $\mathbf{R}(t) = (X, Z) = (b, vt)$ where b is the impact parameter and v is the impact velocity. The interaction with the laser field $\mathbf{E}(t) = \mathbf{E}_0(t) \sin(\omega t + \delta)$ is treated in the dipole approximation and in velocity gauge. The time-dependent Hamiltonian then reads (atomic units are used throughout)

$$H(t) = \frac{\mathbf{p}^2}{2} + \mathbf{p} \cdot \mathbf{A}(t) + V(\mathbf{r}_t) + V(\mathbf{r}_p), \quad (1)$$

where $\mathbf{A}(t) = -\int_0^t \mathbf{E}(t') dt'$, $\mathbf{r}_t = \mathbf{r} + \mathbf{R}(t)/2$, and $\mathbf{r}_p = \mathbf{r} - \mathbf{R}(t)/2$. For the electron-proton interaction V we use the softcore potential from Ref. [13]. For the laser field, we choose a wavelength of 800 nm and an intensity of 1×10^{14} W/cm² since these parameters are readily available in experiment. We use a trapezoidal pulse shape with a three-cycle turn on and turn off. The total pulse duration is 16 optical cycles, which is equal to 42.7 fs.

Initially, the electron is in the ground state of the target atom, i.e., localized around $\mathbf{r}_t = 0$. The time-dependent Schrödinger equation is then solved numerically by means of the split-operator method [14]. The initial distance between target and projectile is set to $\mathbf{R}_0 = (b, -250$ a.u.) so that the closest approach occurs at mid-pulse.

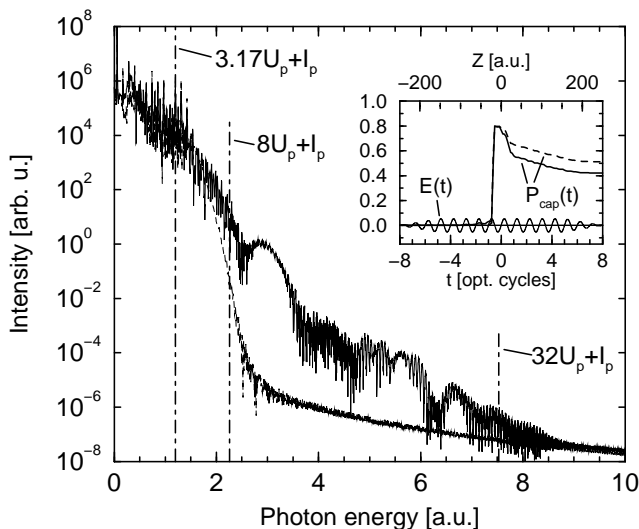


FIG. 1: Emission spectra for impact parameter $b = 4$ a.u. and laser phase $\delta = 0$. Full curve: polarization axis parallel to impact velocity. Dashed curve: polarization axis perpendicular to impact velocity. The vertical lines indicate the position of cutoff energies for various mechanisms (see text). The inset shows the time-dependence of the laser field and the capture probability for the two polarization directions.

The HHG spectrum is calculated according to [15]

$$S(\omega) \sim \left| \int \langle \mathbf{a}(t) \rangle e^{i\omega t} dt \right|^2, \quad (2)$$

where $\langle \mathbf{a}(t) \rangle$ is the time-dependent dipole acceleration vector.

Figure 1 shows the harmonic spectrum obtained for a collision with impact parameter $b = 4$ a.u. and phase $\delta = 0$ of the laser. The two curves correspond to different directions of the laser polarization. If the polarization axis is perpendicular to the impact velocity, the emission spectrum has a form which is familiar from HHG in isolated atoms: a cutoff occurs at the photon energy $3.17U_p + I_p$. Apparently, the passing projectile does not change the cutoff energy. If the polarization axis is parallel to the impact velocity, the result is strikingly different. We find an extension of HHG to frequencies reaching slightly beyond $32U_p + I_p$. The region between $3.17U_p + I_p$ and $8U_p + I_p$ appears like an extension of the atomic plateau with a steeper slope. (The significance of the values $8U_p$ and $32U_p$ will be explained below.) Furthermore, interesting hump structures appear in the spectrum around 3 a.u., 5.6 a.u., and 6.6 a.u.

The inset of Fig. 1 shows the electric field $E(t)$ and the capture probability $P_{\text{cap}}(t)$ which we define as the probability that the electron is found within a square of size 40×40 a.u. around the projectile. We see that the duration of the collisional capture process is much shorter than the pulse length since the ion-atom colli-

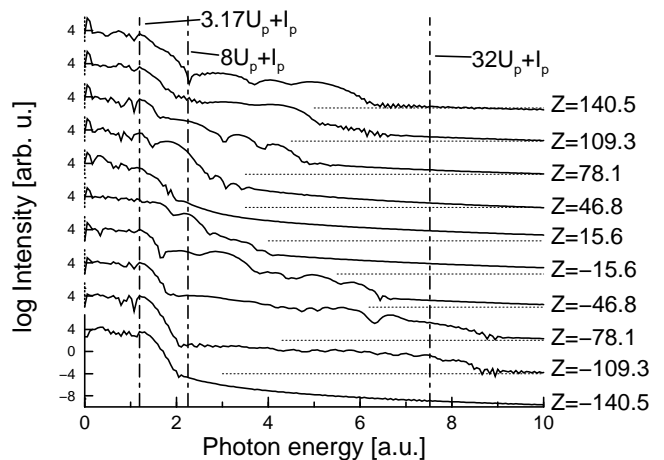


FIG. 2: Temporal analysis of harmonic emission for the same parameters as in Fig. 1. The polarization axis is parallel to the impact velocity. Each spectrum describes the emission during one laser cycle and the value $Z = vt$ refers to the middle of the respective time interval. The dotted horizontal lines indicate the respective level of $\log I = -10$. The vertical lines indicate the same cutoff energies as in Fig. 1

sion is essentially an attosecond process, cf. [7]. After capture at mid-pulse, P_{cap} decreases due to ionization in the strong field. The capture probability is smaller for the case where the laser polarization is along the impact velocity, indicating that this geometry leads to more ionization during the ion-atom collision.

Figure 2 gives a temporal analysis of the harmonic emission for the case that the laser is polarized parallel to the impact direction. Each spectrum in the figure is obtained by Fourier transforming the dipole acceleration over one laser cycle. We find that the emission below the atomic cutoff is nearly independent of time. The situation is not the same for the higher harmonics. Initially, there is no emission of ultrahigh harmonics ($Z = -140.5$ a.u.). Nevertheless, harmonics up to the highest frequency are produced already at $Z = -109.3$ a.u. and $Z = -78.1$ a.u., i.e. long before the actual ion-atom collision. Around $Z = 0$, the emission at the highest frequencies is weak. Instead, harmonics up to $8U_p + I_p$ are generated. At later times, emission at these energies drops and again, higher frequencies are produced. It is evident that the spectral structures at 3 a.u., 5.6 a.u., and 6.6 a.u. in Fig. 1 mainly arise from emission around $Z = -46.8$ a.u. and $Z = -78.1$ a.u. Since the generation of these harmonics is limited to almost only one laser cycle, individual harmonics are not well resolved in those parts of the spectrum. The fact that ultrahigh harmonics are already generated at times when the approaching ion is farther than 100 a.u. from the target clearly shows that the presence of the ion influences the dynamics of the laser-driven electrons when

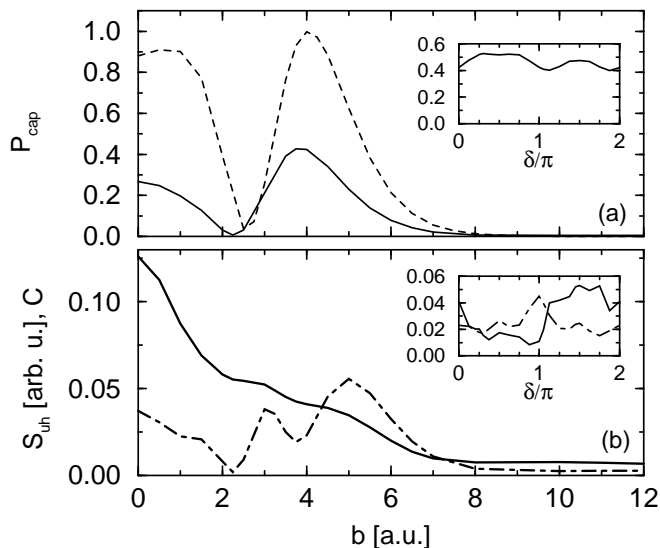


FIG. 3: Panel (a): full curve, capture probability versus impact parameter for a laser field with phase $\delta = 0$; dashed curve, field-free capture probability. Panel (b): yield of ultrahigh harmonics (full curve) and coherence parameter (dot-dashed curve) versus impact parameter. The polarization axis is parallel to the impact velocity. The insets show the same quantities as a function of the laser phase δ for fixed impact parameter $b = 4$ a.u.

they are *far away from the target atom*.

As the next step in our analysis, we vary the impact parameter while keeping all other parameters constant. Figure 3(a) displays the final capture probability P_{cap} as a function of the impact parameter, with and without the presence of the laser. The capture probability is significantly reduced by strong-field ionization. The oscillatory dependence on the impact parameter, however, is qualitatively unchanged.

Since we are particularly interested in harmonic generation well beyond the atomic cutoff, we define the yield of ultrahigh harmonics as the integrated quantity

$$S_{\text{uh}} = \int_{5U_p + I_p}^{\infty} S(\omega) d\omega. \quad (3)$$

The solid line in Fig. 3(b) displays the yield of ultrahigh harmonics as a function of the impact parameter. Its overall structure is a monotonic decrease. Thus, at first sight it exhibits no correlation with the capture probability. A closer look, however, reveals that the “dips” around $b = 2.5$ a.u. and $b = 4$ a.u. coincide with extrema of the capture probability. For further investigation of this point we define the coherence parameter C according to $C = P_{\text{cap}} P_t$. Here, P_t is the final probability that the electron remains bound to the target atom, and is calculated analogous to P_{cap} . Small values of C indicate either ionization or that the electron is localized at one of

the two nuclei. For large values of C , the electron state is a coherent superposition of target and projectile states. Figure 3(b) shows that the maxima of C coincide with shoulders in S_{uh} while the minima in C coincide with the dips in S_{uh} .

We conclude that the generation of harmonics beyond the atomic cutoff originates from at least two different mechanisms. One mechanism is unrelated to the coherence parameter and gives rise to the monotonic decreasing background in Fig. 3(b). A second mechanism depends on the strength of the coherence parameter and gives rise to the oscillations on top of the background.

The insets in Fig. 3 show the dependence on the laser phase δ for fixed impact parameter $b = 4$ a.u. As we vary the phase, we find only modest changes in the capture probability, but a significant alteration of S_{uh} . Note that phases between π and 2π give a higher yield than phases between 0 and π . No clear correlation with the coherence parameter C is observed, indicating that the first mechanism dominates. This is consistent with the smallness of the coherence parameter at $b = 4$ a.u.

As an explanation of our results, we propose the following two mechanisms of HHG. In mechanism (i), one of two collision partners is ionized by the laser, the free electron is then accelerated in the time-dependent laser field, and finally the electron recombines with the *other* ion. Mechanism (ii) also begins with the creation and acceleration of a free electron. Instead of recombining at the other ion, however, the electron is elastically reflected and is further accelerated in the laser field before it finally recombines with the core from which it was originally ejected.

Some years ago, mechanism (i) has been suggested as a new mechanism of HHG in stretched molecules [16, 17, 18], and a cutoff at $8U_p + I_p$ was derived for the special internuclear distances $R = (2n + 1)\pi\alpha$, $n = 0, 1, \dots$, where $\alpha = E_0/\omega^2$ is the classical quivering amplitude of the laser-driven electron. Until now, this cutoff has not been observed in experiment. One reason seems to be that rather large internuclear distances are required. Moreover, the effect occurs only for systems where the state of the electron prior to ionization can be described by a single-particle orbital that is coherently delocalized over both nuclei. For example, this is a valid description for the ground-state of an H_2^+ molecular ion, but not for a neutral molecule at large internuclear distances. In an ion-atom collision, a coherent superposition is realized if the coherence parameter C is appreciable. This explains the connection between C and S_{uh} in Fig. 3(b).

Under the assumption of fixed nuclei, it is straightforward to derive the maximum cutoff for both processes by inspection of the classical electronic equation of motion, $\dot{\mathbf{i}} = -\mathbf{E}_0 \sin \omega t$. For an electron starting with zero

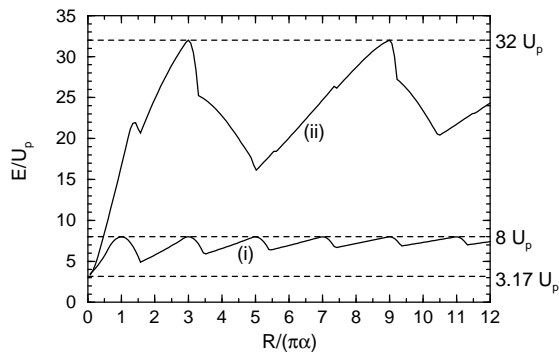


FIG. 4: Maximum kinetic electron energy versus internuclear distance for the recombination of a laser-driven electron in mechanisms (i) and (ii), see text (classical calculation for fixed nuclei).

velocity at $\mathbf{r} = 0$ at time t_0 , we have

$$\dot{\mathbf{r}}(t) = (\mathbf{E}_0/\omega)(\cos\omega t - \cos\omega t_0). \quad (4)$$

Thus, the largest possible velocity equals $2E_0/\omega$, corresponding to an energy of $8U_p$. If an electron with this energy recombines at the other ion, it will generate a photon with energy $8U_p + I_p$. This explains the cutoff law for mechanism (i). If the electron is instead elastically backscattered at time t_1 , the velocity is thereafter given by

$$\dot{\mathbf{r}}(t) = (\mathbf{E}_0/\omega)(\cos\omega t + \cos\omega t_0 - 2\cos\omega t_1), \quad t > t_1, \quad (5)$$

so that the maximum velocity is $4E_0/\omega$ corresponding to an energy of $32U_p$. This maximum occurs for the case that t_0 , t_1 , and t are times of zero electric field. It is straightforward to show that recollision with the maximum energy is possible if the internuclear distance satisfies the condition $R = 3(2n+1)\pi\alpha$, $n = 0, 1, \dots$. Therefore, at these distances we have a cutoff at $32U_p + I_p$. For the present laser parameters, $\alpha = 16.5$ a.u. and $U_p = 0.22$ a.u. Although nonzero ion velocities may lead to a correction of the cutoff, we conclude that the generation of ultrahigh harmonics (Figs. 1,2) is well explained by the reflection mechanism.

For mechanisms (i) and (ii), Fig. 4 shows the maximum electron energy at recombination time as a function of the internuclear distance. These results are obtained by numerical solution of the classical equation of motion for fixed nuclei. Both curves approach the atomic limit $3.17U_p$ for $R \rightarrow 0$. The maximum energies are found at $32U_p$ and $8U_p$, respectively, and this gives rise to the cutoffs mentioned above. Note also that already at $R = \pi\alpha$, the reflection mechanism produces electron energies above $16U_p$.

The phase dependence observed in Fig. 3 is consistent with the reflection scenario due to the asymmetry of the

ion-atom system. Before the ion-atom collision, reflection of electrons can occur only for electrons that are accelerated from the target towards the projectile. Under inversion of the field direction (phase shift by π), these electrons are accelerated in the opposite direction where they cannot be backscattered.

In summary, we have investigated ion-atom collisions in the presence of a strong laser field. High harmonics are generated with energies much larger than found in atomic HHG if the laser polarization axis is parallel to the direction of impact. We have proposed two distinct HHG mechanisms, both involving laser-driven transfer of electrons between the collision partners. The highest harmonics are produced by reflection of electrons from the projectile back to the target atom at times when target and projectile are far away from each other. A simplified classical description of the electron gives a cutoff energy at $32U_p + I_p$ for this process. In principle, the mechanisms of HHG that we have discussed should appear also in molecules. However, it seems difficult to combine the required large internuclear distances with precise control of the molecular orientation. In ion-atom collisions, all possible distances are sampled, and the orientation control is straightforward.

-
- [1] R. Dörner *et al.*, Phys. Rep. **330**, 95 (2001).
 - [2] M. Protopapas, C. H. Keitel, and P. L. Knight, Rep. Prog. Phys. **60**, 389 (1997).
 - [3] P. Lambropoulos, P. Maragakis, and J. Zhang, Phys. Rep. **305**, 203 (1998).
 - [4] A. Débarre and P. Cahuzac, J. Phys. B **19**, 3965 (1986).
 - [5] G. Ferrante, L. L. Cascio, and B. Spagnolo, J. Phys. B **14**, 3961 (1981); T. S. Ho, C. Laughlin, and S. I. Chu, Phys. Rev. A **32**, 122 (1985); Y. P. Hsu and R. E. Olson, Phys. Rev. A **32**, 2707 (1985); C. Chaudhuri and T. K. Rai Dastidar, Nuovo Cimento D **20**, 749 (1998); A. B. Voitkiv and J. Ullrich, J. Phys. B **34**, 1673 (2001); S.-M. Li, J. Chen, and Z.-F. Zhou, J. Phys. B **35**, 557 (2002).
 - [6] L. B. Madsen, J. P. Hansen, and L. Kocbach, Phys. Rev. Lett. **89**, 093202 (2002).
 - [7] T. Kirchner, Phys. Rev. Lett. **89**, 093203 (2002).
 - [8] A. McPherson *et al.*, J. Opt. Soc. Am. B **4**, 595 (1987).
 - [9] P. Agostini, F. Fabre, G. Mainfray, G. Petite, and N. K. Rahman, Phys. Rev. Lett. **42**, 1127 (1979); J. H. Eberly, J. Javanainen, and K. Rzążewski, Phys. Rep. **204**, 331 (1991).
 - [10] C. Spielmann *et al.*, Science **278**, 661 (1997).
 - [11] A. Paul *et al.*, Nature **421**, 51 (2003).
 - [12] P. B. Corkum, Phys. Rev. Lett. **71**, 1994 (1993).
 - [13] M. Protopapas, D. G. Lappas, and P. L. Knight, Phys. Rev. Lett. **79**, 4550 (1997).
 - [14] M. D. Feit, J. A. Fleck, Jr., and A. Steiger, J. Comput. Phys. **47**, 412 (1982).
 - [15] K. Burnett, V. C. Reed, J. Cooper, and P. L. Knight, Phys. Rev. A **45**, 3347 (1992).
 - [16] P. Moreno, L. Plaja, and L. Roso, Phys. Rev. A **55**, R1593 (1997).

- [17] A. D. Bandrauk, S. Chelkowski, H. Yu, and E. Constant, Phys. Rev. A **56**, R2537 (1997). 4022 (1998).
- [18] R. Kopold, W. Becker, and M. Kleber, Phys. Rev. A **58**,